Kinetics and Isotherm of Block Copolymer Adsorption on Latex Particles. Part 1[1]

Renliang Xu* and Greg D'Unger

Scientific Instruments, Coulter Corporation, 1950 West 8th Avenue, Hialeah, Florida 33010

Mitchell A. Winnik

Department of Chemistry and Erindale College, University of Toronto, 80 St. George St., Toronto, Ontario, Canada M5S 1A1

J. M. G. Martinho and J. M. R. d'Oliveira

Centro de Quimica-Fisica Molecular, Instituto Superior Tecnico, Av. Rovisco Pais, 1096 Lisboa Codex, Portugal

Received February 22, 1994. In Final Form: June 2, 1994®

Polystyrene–poly(ethylene oxide) (PS-PEO) block copolymers form micelles in aqueous solution. When the solution is mixed with a dispersion of polystyrene latex spheres (PSL) in suspension, adsorption of copolymer molecules onto latex particles takes place. The adsorption changes the physical dimension and the surface characteristics, such as ζ potential, of the particles. Electrophoretic light scattering is used to investigate the adsorption kinetics by measuring mobilities and mobility changes of PSL in the mixtures. The mobility of PSL is decreased after PS-PEO copolymers adsorption due to surface potential reduction at the shear layer. Analysis of the electrophoretograms reveals that there are several kinetics processes for the surface rearrangement of the polymer chains on the surface after adsorption, depending upon the mixing ratio and the curvature of the PSL particles. On the basis of the present observations a three-step kinetic mechanism is proposed.

Introduction

In recent decades, the phenomena associated with polymer adsorption onto surfaces have attracted much attention both theoretically and experimentally. Pioneered by Alexander and de Gennes, several theories have been developed dealing with molecular conformation after adsorption in different situations, ranging from adsorption of homopolymer in good solvent onto a flat solid wall or onto a rough surface to block copolymer adsorption in selective solvents, either in micelle form or in unimer form.[2-5] All models are formulated under the scaling law scheme for polymers in a dilute noncharged environment. There are few publications that take into account the effect of surface curvature. Some current theories also consider adsorption kinetics for single-molecule processes.[6]

Most experimental studies to date on polymer adsorption kinetics have been limited to adsorption onto flat surfaces. These experiments have relied on ellipsometry, neutron reflectometry, and surface plasmon measurements by which online adsorption processes can be observed and monitored.[7-9]

We have used dynamic light scattering and size exclusion chromatography to investigate indirectly aspects of the kinetics of adsorption of block copolymers onto small polystyrene latex (PSL) microspheres in a selective solvent, in which the block copolymers exist mainly in the micelle form. We found that the adsorption process involves direct adsorption of micelles onto the surface of the PSL particles, followed by a rearrangement process that is surface-curvature sensitive. On the basis of these observations we proposed a kinetic micelle adsorption model that, for the first time, takes the curvature of the interface as one of the primary factors in the adsorption process.[10,11]

In the present study we apply electrophoretic light scattering to investigate the adsorption kinetics of PS-PEO block copolymers onto PSL particles in aqueous suspension by monitoring the electrophoretic mobility change of the PSL particles. These changes are a direct consequence of surface modification due to adsorption of block copolymers. We observed a fast initial adsorption followed by a slow process. The slow process may involve more adsorption and surface rearrangement of adsorbed molecules. The adsorption process is sensitive to the curvature of the PSL particles. In addition, by analyzing the electrophoretograms of various mixtures, we find that there are two distinct adsorption conformations in each mixture. On the basis of these observations we propose a three-step kinetic mechanism for our direct micelle-adsorption model.

Experimental Section

Poly(ethylene oxide)–polystyrene diblock copolymers, courtesy of Z. Hruska, G. Hurtrez, and G. Riess, Mulhouse, France, were synthesized by standard anionic polymerization in THF solution

* To whom all correspondence should be addressed.

® Abstract published in *Advance ACS Abstracts*, August 1, 1994.

(1) Paper No. 8 in a series on block copolymer in solution.

(2) Lee, L. H. *Adhesion and Adsorption of Polymers*; Plenum Press: New York, 1980.

(3) Napper, D. H. *Polymeric Stabilization of Colloid Dispersions*; Academic Press: London, 1975.

(4) For a review, see: Halperin, A.; Tirrell, M.; Lodge, T. P. *Adv. Polym. Sci.* **1991**, *100*, 1.

(5) Marques, C.; Joanny, J. F.; Leibler, L. *Macromolecules* **1988**, *21*, 1051.

(6) (a) Johner, A.; Joanny, J. F. *Macromolecules* **1990**, *23*, 5299. (b) Kislenko, V. N.; Berlin, Ad. A.; Moldovanov, M. A. *Kolloidn. Zh.* **1993**, *55(1)*, 83.

(7) Munch, M. R.; Gast, A. *J. Chem. Soc. Faraday Trans.* **1990**, *86*, 1341.

(8) Munch, M. R.; Gast, A. *Macromolecules* **1990**, *23*, 2313.

(9) Motschmann, H.; Stamm, M.; Toprakcioglu, Ch., *Macromolecules* **1991**, *24*, 3681.

(10) Xu, R.; d'Oliveira, J. M. R.; Winnik, M. A.; Riess, G.; Croucher, M. D. *J. Appl. Polym. Sci. Appl. Polym. Symp.* **1992**, *51*, 135.

(11) d'Oliveira, J. M. R.; Xu, R.; Jensma, T.; Winnik, M. A.; Hruska, Z.; Hurtrez, G.; Riess, G.; Martinho, J. M. G.; Croucher, M. D. *Langmuir* **1993**, *9*, 1092.

0743-7463/94/2410-2977$04.50/0

Table 1. Summarized Properties of PS-PEO Copolymer in Water

sample	M_{PEO} (g/mol)	M_{total} (g/mol)	M_w/M_n (g/mol)	G (μS/cm)	μ (μm·cm/V/s)	$M_{micelle}$ (g/mol)
ZGH3	11 000	15 000	1.20	23	−0.22	2.0×10^6
ZGH4	18 400	22 200	1.17	12	−0.15	2.9×10^6
ZGH5	28 800	32 600	1.25	12	−0.06	4.2×10^6

Table 2. Summarized Properties of PSL Particles in Water

sample	d_{DLS} (nm)	d_{EM} (nm)	G (μS/cm)	μ (μm·cm/V/s)	M^a (g/mol)
L69	64	63	48	−3.38	1.1×10^8
L109C	108	99	20	−3.43	4.2×10^8
L223	223	202	4	−3.30	3.7×10^9

[a] Calculated as if the particles are anhydrous.

using a common living PS block as a precursor. After purification, they were characterized primarily by size exclusion chromatography and by ^{1}H NMR.[12] The three samples have the same styrene block length but different block lengths of ethylene oxide. Table 1 lists the characteristics of the copolymer samples. Micelle solutions of block copolymers were prepared by adding the block copolymer directly into deionized water (Milli-Q grade; c = 1 mg/mL), warming the mixture to 50 °C for 1 h and cooling to room temperature.

PSL particles in concentrated suspensions were gifts from D. S. Mohanraj of Seradyne. One sample (L109C) contains surface carboxyl groups, and the other two, only sulfate groups. The surfactants remaining from the polymerization were not removed. Table 2 lists the sizes of the latex particles in suspension characterized by dynamic light scattering (Coulter N4MD) and by electron microscopy. The dispersions were diluted with deionized water to a concentration of 1 mg/mL. No control ions were added during preparation of the micelle solutions and dilution of the PSL suspensions.

Particle mobilities were measured by electrophoretic light scattering using a Coulter DELSA 440 instrument. The DELSA 440 is a multi-angle heterodyne electrophoretic light scattering apparatus capable of making simultaneous measurements at four different scattering angles with a wide range of electric field strengths.

Electrophoretic Light Scattering

Electrophoretic light scattering is an emerging technique for studying or characterizing charged macromolecules such as proteins and synthetic polyelectrolytes and particles such as lattices and metal oxides.[13,14] In an electrophoretic light scattering measurement, the scatterers in solution are illuminated by a polarized coherent laser light and scatter light. The frequency of the scattered light is slightly different, a few hundred hertz, from that of the incident light due to the Doppler effect from random Brownian motion and electrophoretic motion of the scatterers along the applied electric field direction. When the scattered light is mixed with a portion of the coherent incident light, often called the reference beam, the frequency difference between the two light beams is detected. From this signal, particle size and surface potential information are retrieved.[15]

The spectrum obtained from an electrophoretic light scattering measurement of a sample of both polydisperse size and polydisperse mobility is

$$S(w) = A + B\int_{\mu_{max}}^{u_{min}}\int_{\Gamma_{max}}^{\Gamma_{min}} \frac{I(u,r)\,\Gamma(r)}{(w \mp (w_s + u))^2 + (\Gamma(r))^2}\,d\Gamma\,du \quad (1)$$

where A and B are two constants for the baseline and normalization, respectively. $\Gamma(r)$ is the characteristic linewidth due to the Brownian motion; I(u,r), the scattered intensity; u, the frequency shift caused by mobility; w_s, a preshifting frequency for the illuminating beam in order to distinguish the moving direction of the scatterers from the spectrum; and r, the particle radius. Equation 1 is reduced to a simple Lorentzian form for monodisperse samples:

$$S(w) = A + \frac{B\Gamma}{(w \mp (w_s + u))^2 + \Gamma^2} \quad (2)$$

For a spherical particle, Γ, in units of hertz is related to its radius r through the Stokes–Einstein equation:

$$\Gamma = \frac{4k_B T}{3\eta r}\left(\frac{n}{\lambda_0}\sin\left(\frac{\theta}{2}\right)\right)^2 \quad (3)$$

with k_B, T, η, n, λ_0, and θ being the Boltzmann constant, the absolute temperature, the solvent viscosity, the solvent refractive index, the light wavelength in vacuo, and the scattering angle, respectively.

The parameter u is related to the electrophoretic mobility μ of a particle by

$$u = \frac{2\mu E n}{\lambda_0}\sin\left(\frac{\theta}{2}\right)\sin\left(\frac{\theta}{2} + \phi\right) \quad (4)$$

with E and ϕ being the applied electric field strength and the angle between the directions of light propagation and the applied electric field, respectively.

For nonconducting spherical particles, the Henry equation (5) can be used to calculate the ζ potential of a particle from μ, if one assumes that (1) the total electric field a particle experienced in a superposition of the applied field and the field due to the charge of the particle, (2) the distortion of the field induced by the movement of the particle, i.e., the relaxation effect, can be ignored, (3) the inertia terms in the hydrodynamic equation are negligible, and (4) $e\psi/k_BT \ll 1$ (ψ is the potential).

$$\mu = \frac{\zeta\epsilon}{1.5\eta}f(\kappa r) \quad (5)$$

Here ϵ and κ are the permittivity of the electrolyte medium and the Debye–Hückel reciprocal thickness of the double layer surrounding the particle, respectively. The function $f(\kappa r)$ depends on the particle shape, and the analytical form of $f(\kappa r)$ for a sphere is available.[16] $\kappa(\text{nm}^{-1}) = 3.288(^1/_2\Sigma c_i z_i^2)^{1/2}$ in water at 25 °C, with c_i being the concentration of ion i in mol/L and z_i the valence of ion i.

More rigorous relationships between μ and ζ without the above restrictions can be found in the literature.[17–19] However, the calculation of the ζ potential from electro-

(12) Caldérara, F.; Hruska, Z.; Hurtrez, G.; Nugay, T.; Riess, G. *Makromol. Chem.* **1993**, *194*, 1411.
(13) Kosmulski, M.; Matijević, E. *Langmuir* **1991**, *7*, 2006.
(14) Woodle, M. C.; Collins, L. R.; Sponsler, E.; Kossovsky, N.; Papahadjopoulos, D.; Martin, F. J. *Biophys. J.* **1992**, *61*, 902.
(15) Ware, B. R.; Haas, D. D. In *Fast Methods in Physical Biochemistry and Cell Biology*; Sha'afi, R. I., Femandez, S. M., Eds.; Elsevier: New York, 1983; Chapter 8, pp 174–219.
(16) Henry, D. C. *Proc. R. Soc. London* **1931**, *A133*, 106. With a correction, the $f(\kappa r)$ function should read $f(\kappa r) = 1 + (\kappa r)^2/16 - 5(\kappa r)^3/48 - (\kappa r)^4/96 + (\kappa r)^5/96 - [(\kappa r)^4/8 - (\kappa r)^6/96]e^{\kappa r}\int_\infty^{\kappa r} e^{-t}/t\,dt$. When $\kappa r > 25$, $f(\kappa r)$ can be approximated as (to three significant figures) $f(\kappa r) = 3/2 - 9/2\kappa r + 75/2\kappa^2 r^2 - 330/\kappa^3 r^3$.
(17) Wiersema, P. H.; Loeb, A. L.; Overbeek, J. Th. G. *J. Colloid Interface Sci.* **1966**, *22*, 78.
(18) O'Brien, R. W.; White, L. R. *J. Chem. Soc. Faraday Trans. 2* **1978**, *74*, 1607.
(19) Deggelmann, M.; Palberg, T.; Hagenbuchle, M.; Maire, E.; Krause, R.; Graf, C.; Weber, R. *J. Colloid Interface Sci.* **1991**, *143*, 318.

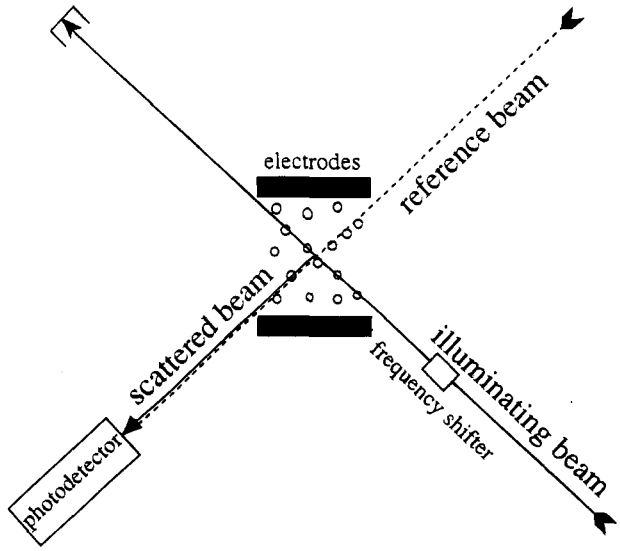

Figure 1. Schematic diagram of the DELSA 440 optics.

phoretic mobilities using these procedures[17,18] requires tedious computation and prior knowledge of some parameters, whose values are often unknown of difficult to obtain. When $\kappa r < 0.01$ or > 200, the ζ potentials calculated from the Henry equation and from the procedures described in refs 17 and 18 are virtually the same. In the range of κr between 1 and 10, there is no unique assignment of ζ to a particular mobility μ. If one uses the Henry equation instead of the rigorous solution, the error in the ζ potential computed due to neglect of the relaxation effect is a function of μ and κr.[17] The error increases monotonically with increasing μ and maximizes when κr reaches around 4.

Figure 1 is a schematic diagram of the optical system used in the DELSA 440. Only one scattering angle and one detector are shown for the sake of clarity. The illuminating beam and the reference beam are from the same He–Ne coherent laser source. However, the frequency of the illuminating beam has been shifted by a small known amount w_s up to 500 Hz by using a moving mirror system. The scattered light, which is Doppler-shifted by a small amount due to the motion of particles in addition to w_s, and the reference beam, which is not Doppler-shifted, are detected by a photodetector. The two beams are mixed at the surface of the photodetector to generate the beating frequency. The signals are first passed into a 256-channel correlator. Power spectra of the dampened sinusoidal signals are then retrieved by Fourier transforms of the autocorrelation functions. The cell used was a rectangular cross section capillary tube with hemispherical silver electrodes at the ends. The cell was thermostated with a Peltier surface. To avoid influence from electroosmotic flow of the liquid, the measurements were performed at either the upper or the lower stationary layers where fluid motion does not contribute to electrophoretic motion of the particles.[20,21] Most of the data were acquired over a time period of 60 s. The polarity of the applied DC electric field was changed every 2 s with a 0.5 s field-off period in between. In the data analysis procedure, we used the data acquired primarily at the lowest scattering angle (8.6°).

Results and Discussion

In the present study, when the Henry equation is used to convert electrophoretic mobilities μ to ζ potentials, the error in the calculated ζ potential is estimated to be about 10% for the PSL particles before adsorption when they have the largest μ value (≈ -3.5 μm·cm/V/s) and to be only a few percent for all the other measurements.[17] However, the application of the Henry equation requires prior knowledge of κr. As we stated above, $f(\kappa r)$ is a monotonically increasing function starting from 1 when $\kappa r = 0$ up to 1.5 when $\kappa r = \infty$. In the present study, the conductivities for the diluted PSL dispersions were quite low (Table 2). The ion concentrations of the dispersions are estimated to be on the order of 10^{-6} weight fraction, according to the conductivities of common ion solutions at different concentrations. Because of the way they were prepared, all latex dispersions and copolymer solutions had very low ionic strengths. We estimate that κr values for the present systems with particle diameters in the range of tens to hundreds of nanometers would be smaller than 10, corresponding to $f(10) = 1.24$. As an approximation, the $f(\kappa r)$ value for the present study was taken to be a constant ($= 1.10$).[22] On the basis of the fact that the mobility change of PSL particles due to adsorption of copolymers was much larger than 10%, this approximation has a negligible effect on our analysis and conclusions. Thus, the measured electrophoretic mobility μ was treated as linearly proportional to the ζ potential (ζ(mV) = 17.5 μ (μm·cm/V/s)) within the experimental error limit under the above approximation.

The neutral copolymer molecules in micelle form had very small mobilities (Table 1). The mobilities are likely due to ionic residues left from the anionic synthesis of the copolymers. We note that the copolymer with the highest repeating PEO unit (ZGH5) had the lowest mobility in solution. Although L69 and L223 contain sulfate groups on the surface and L109C contains surface carboxylate groups, their ζ potentials and mobilities were the same. When a copolymer micelle solution was added to a PSL dispersion, the mobility of the mixture decreased immediately, and the mobility distribution was broadened. The mobility of the mixture depended on the diameter of the PSL particles, the copolymer chain length, and the mixing ratio. In addition, the mobility evolved with time before it reached an equilibrium. In our experiments, the difference in the PSL's surface groups does not show noticeable effects on their adsorption behaviors.[11]

Time Dependence. We observed a two-stage dynamic ζ potential evolution process for all mixtures. The electrophoretogram of the mixture was never found to be a simple addition of the electrophoretograms of the PSL dispersion (a peak at around -3.5 μm·cm/V/s) and that of copolymer solution (a peak at around -0.2 μm·cm/V/s), even for the measurements performed as soon as 3 min after mixing. The electrophoretogram of the mixture changed continuously from its initial shape until it stabilized, usually within an hour. Depending on the PSL diameter, the copolymer chain length, and their mixing ratio, there were three types of electrophoretograms. In some systems, referred to as "type I", the mobility distribution appeared initially in the form of a broad peak covering a range from around zero to ~ -3.5 μm·cm/V/s. This broad, multishouldered peak shrank continuously until it became a slim single peak. Figure 2 shows a typical mobility variation as a function of time for a 1:1 mixture of ZGH3 solution and L69 dispersion from 3 min after mixing until 70 min. The type II process started with a

(20) Haas, D. D. Ph.D. Dissertation, Harvard University, 1978.
(21) Kosmuski, M.; Matijevic, E. *Colloid Surf.* **1992**, *64*, 57.

(22) κr values can be estimated from eq 7 if one knows the adsorption layer thickness Δ. Taking Δ values from ref 11 and assuming $z = 2$, we found that $(\kappa r)_{L69}$ is equal to 1.60 (from ZGH4 adsorption) or 1.63 (from ZGH5 adsorption), and $(\kappa r)_{L109C}$ is equal to 4.53 (from ZGH4 adsorption) or 5.08 (from ZGH5 adsorption) with corresponding $f(1.6) = 1.05$ and $f(5) = 1.16$.

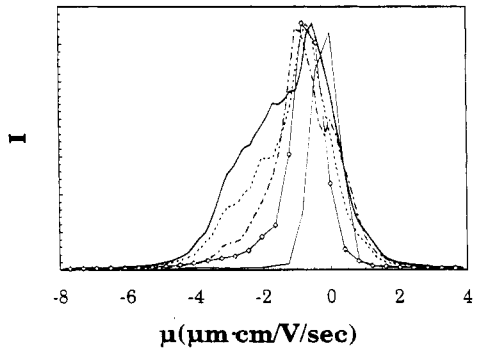

Figure 2. Electrophoretograms of a mixture of ZGH3 solution and L69 suspension at different times after mixing. The mixing weight ratio is 1:1. The acquisition time after mixing and the applied field strength for the symbols are as follows: (solid line) 3 min after mixing, ±37.6 V/cm; (dotted line) 10 min, ±37.6 V/cm; (dashed line) 37 min, ±37.6 V/cm; (diamonds connected by a thin solid line) 70 min, ±15.7 V/cm. The thin solid line is from a pure ZGH3 solution with a ±15.7 V/cm electric field plotted for comparison.

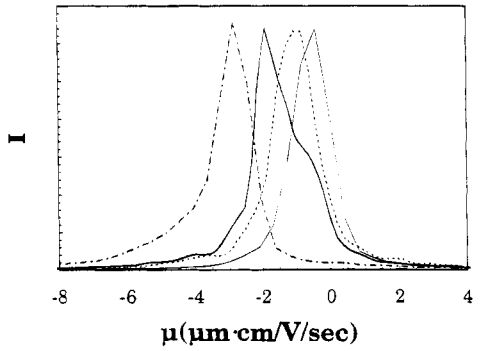

Figure 3. Electrophoretograms of a mixture of ZGH4 solution and L69 suspension at different times after mixing. The mixing weight ratio is 1:1. The data were acquired under a ±15.7 V/cm electric field: (solid line) acquired 5 min after mixing; (dotted line) 20 min after. The thin solid line is from a pure ZGH4 solution, and the dashed line is from a pure L69 suspension for comparison.

single peak with a shoulder at the lower mobility side. When it reached a stable shape, the shoulder grew to a peak, and the original peak at the higher mobility side disappeared. Figure 3 shows the mobility variation for a mixture of ZGH4 solution and L69 dispersion as an example of this type of process. The type III phenomenon displayed two distinguished peaks at all times. However, the ratio of the two peaks changed with time, favoring the lower mobility peak. The mobilities of both peaks were lower than that of bare PSL particles but higher than that of neutral copolymer micelles. Figure 4 displays two electrophoretograms from the mixture of a ZGH3 solution with a L223 dispersion acquired at different times. The time dependence of the three types of electrophoretograms reflect the ζ potential population reorganizing process. In the type I process, there might be particles with different ζ potentials, i.e., a broad ζ potential distribution at the beginning. After more adsorption and surface rearrangement, all particles end up with similar ζ potentials, i.e., with a narrow distribution. In the type II and the type III processes, there appear to be two discrete populations of ζ potentials. The high ζ potential particles convert continuously to particles having lower ζ potentials until they reach equilibrium. Depending on the difference in ζ potentials, small or large, of the two groups and the completeness of the conversion, one observes type II or type III electrophoretograms.

For stabilized mixtures we observed two types of

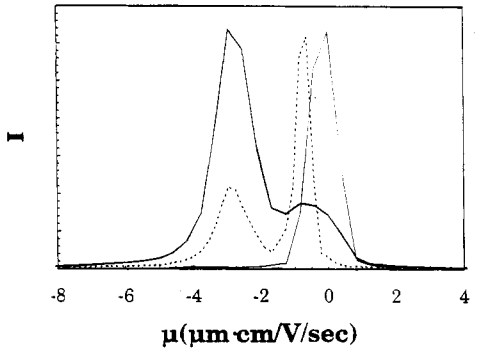

Figure 4. Electrophoretograms of a mixture of ZGH3 solution and L223 suspension at different times after mixing. The mixing weight ratio is 1:1. The data were acquired under a ±15.7 V/cm electric field: (solid line) acquired 5 min after mixing; (dotted line) 5 h after. The thin solid line is from a pure ZGH3 solution for comparison.

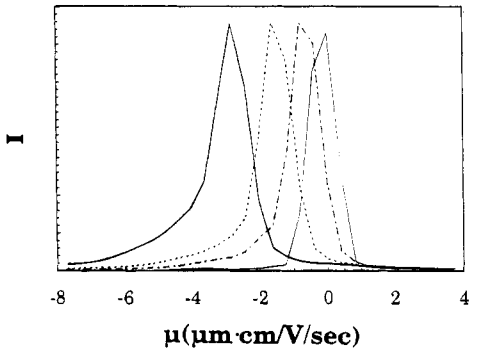

Figure 5. Electrophoretograms of ZGH3 and L69 mixtures at different mixing ratios after equilibrium. The data were acquired under a ±15.7 V/cm electric field. The weight percentages of the PSL particles are solid line, 100%; dotted line, 79%; dashed line, 55%; and thin solid line, 0%.

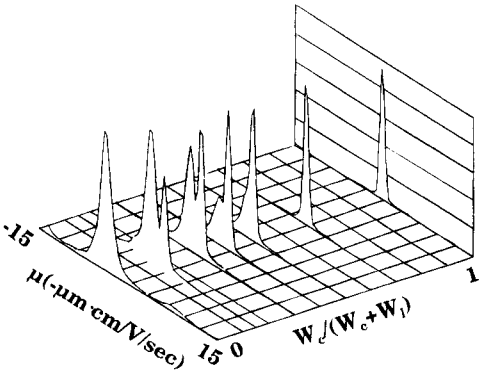

Figure 6. 3-D plot for electrophoretograms of ZGH3 and L109C mixtures of different mixing ratios after equilibrium. The data were acquired under a ±15.7 V/cm electric field.

electrophoretograms. One type had a single peak, and the other type had two peaks. Both the peak location and peak ratio between two peaks were functions of mixing components and mixing ratio. Figure 5 and Figure 6 demonstrate the two types of electrophoretograms as a function of mixing ratio. Figure 5 is from the mixture of a ZGH3 solution and a L69 dispersion at different mixing ratios. Figure 6 is a 3-D plot of mixing ZGH3 solution with L109C dispersion at different mixing ratios $W_c/(W_c + W_l)$, with W_c and W_l being the copolymer solution weight and the latex dispersion weight in the mixture, respectively. In Figure 6, for the higher mobility peak not only is the intensity reduced but also is the location shifted to lower mobility, while the lower mobility peak remains at

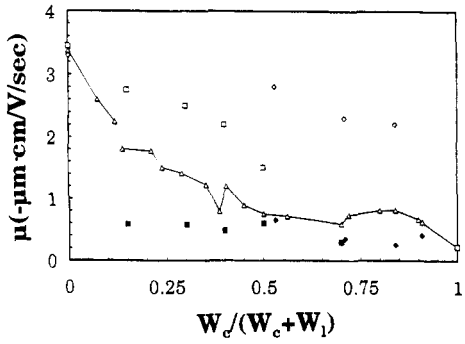

Figure 7. Electrophoretic mobilities of ZGH3 solutions mixed with PSL suspensions at different mixing ratios after equilibrium: (hollow triangles) mixed with L69 suspensions; (hollow and filled squares) the higher mobility peak and the lower mobility peak when mixed with L109C suspensions, respectively; (hollow and filled diamonds) the higher mobility peak and the lower mobility peak when mixed with L223 suspensions, respectively.

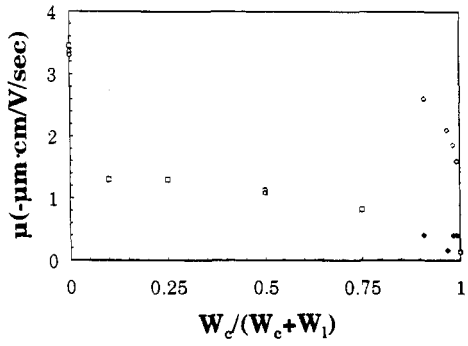

Figure 8. Electrophoretic mobilities of ZGH4 solutions mixed with PSL suspensions at different mixing ratios after equilibrium: (hollow triangles) mixed with L69 suspensions; (hollow squares) mixed with L109C suspensions; (hollow and filled diamonds) and higher mobility peak and the lower mobility peak when mixed with L223 suspensions, respectively.

the same position (higher than that of pure ZGH3 solution) as the percentage of ZGH3 solution in the mixture is increased.

There is a systematic trend for the mobility distribution types and mobility peak locations when we take a close look at the nine mixtures. For the L69 particles, there is always a single peak in the mixing with any one of the three copolymers in any ratio. In Figure 7, the titration curve of L69 dispersion with ZGH3 solution (triangles) shows the peak shifting to a lower mobility as the ZGH3 solution percentage increases until it reaches a plateau at $W_c/(W_c + W_l)$ around 0.5 ($\mu \approx -0.7$ μm·cm/V/s). For the L109C particles, there is a single peak in mixing with ZGH4 or ZGH5 solutions. But it has a single peak when mixed with ZGH3 only at mixing ratios higher than 0.5. For the L223 particles, there are always two peaks for the three copolymer mixtures even when the mixing ratio is very close to 1 where there are very few PSL particles mixed with excess copolymers. One important observation for two-peak electrophoretograms is that the higher mobility peak always shifts to lower mobility with an intensity reduction with increasing percentage of copolymer solution in the mixture, while the location of the lower mobility peak remains basically unchanged. Figures 7–9 display the peak locations for the nine mixtures at different mixing ratios. One feature of Figure 7 is that, for the same copolymer, the larger the PSL particles, the higher the mobility for the higher mobility peak (hollow symbols) at the same mixing ratio. There are not sufficient data to identify this feature in Figures 8 and 9.

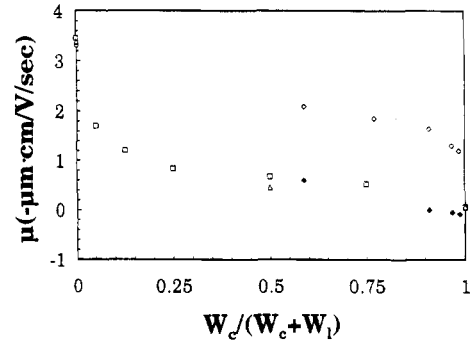

Figure 9. Electrophoretic mobilities of ZGH5 solutions mixed with PSL suspensions at different mixing ratios after equilibrium: (hollow triangles) mixed with L69 suspensions; (hollow squares) mixed with L109C suspensions; (hollow and filled diamonds) the higher mobility peak and the lower mobility peak when mixed with L223 suspensions, respectively.

Factors Affecting Mobility Measurements. Before we discuss copolymer adsorption, we must first examine several factors that influence the electrophoretic mobility measurements. Since the ζ potential of a particle is determined by the particle surface charge density and the surrounding ion concentration and type, any change in solution conductivity will alter a particle's ζ potential. As listed in Table 1, the PSL suspensions and the copolymer solutions all have different conductivities ranging from 4 to 48 μS/cm. There was no attempt to control or to adjust the solution conductivity when two samples were mixed, resulting in mixtures that had different conductivities between 4 and 48 μS/cm, depending upon which two samples were mixed and their mixing ratio. Thus, even without adsorption, the ζ potential of the PSL particles would have been changed. There are several detailed reports in the literature on the electrophoretic mobility of carboxyl PSL and sulfate PSL particles of different diameters as functions of total particle concentration, solution conductivity, and small ion concentration (or pH).[19,23] The variations of electrophoretic mobility are all different, depending on the particular type of particles. However, in the present study, the mobility change that originated from the conductivity change (e.g., from 48 to 19 μS/cm, which represents the largest conductivity change) is very small. We estimate that typically being smaller than 5% from Figure 4 of ref 19. In addition, in the over 100 measurements made from different mixtures in the present study, we did not find correlation between solution conductivity and measured mobility.

PS-PEO copolymers form micelles in water with an average aggregation number related only to the PS block length.[24] This result is in accord with theoretical models.[4] Since the three copolymer samples have the same PS block length, their aggregation numbers should be the same. The aggregation number is estimated to be 130 on the basis of our previous measurements of similar systems.[24] The corresponding micellar weight is then on the order of 10^6 g/mol. On the other hand, the PSL particles are much heavier, with particle weights on the order of 10^8–10^9 g/mol. The intensity of light scattered in the Rayleigh–Debye–Gans limit at a small angle is related to the properties of the scatterer, such as the weight (M_w), the concentration (C), the refractive index (n), and the refractive index increment (dn/dc):

(23) Prescott, J. H.; Shiau, S.-j; Rowell, R. L. *Langmuir* **1993**, *9*, 2071.

(24) Xu, R.; Winnik, M. A.; Riess, G.; Chu, B.; Croucher, M. D. *Macromolecules* **1992**, *25*, 664.

$$I \propto n^2\left(\frac{dn}{dc}\right)^2 M_w C \tag{6}$$

Besides the large mass difference between the PSL particles and the PEO-PS copolymer micelles, polystyrene has a higher n_{PS} (= 1.583) and $(dn/dc)_{PS}$ (= 0.241) when compared with poly(ethylene oxide) (n_{PEO} = 1.456 and $(dn/dc)_{PEO}$ = 0.134).[25] Thus, in the mixture, the detection is almost blind to the copolymer micelles and the unimers. Even for the mixture with the highest copolymer percentage (99.2 wt %), we can estimate that less than 3% of the total light scattered could originate from the micelles, even if there was no micelle adsorption.

One feature that can obscure interpretation of the recorded electrophoretograms, however, is that peak widths are broadened partially due to the embedded Brownian motion of the particles as explained by eq 1 and eq 2. For systems with polydisperse mobilities and polydisperse sizes, there is no analytical solution to deconvolute the Brownian motion from the electrophoretic motion, although approximate methods have been recently proposed.[26] For samples with monodisperse mobility, the peak width is reciprocally proportional to the particle size (eq 3). In the present study, the broad peaks, e.g., the peaks in Figure 2, during the dynamic evolution process are clearly attributable to the mobility- and particle-size inhomogeneity. For the equilibrated mixtures, the peak width would be more indicative of the particle size if we assume that the mobility distribution is narrow.

When flexible neutral polymers are attached to a latex surface, several aspects of their properties affect the measured ζ potential. The two major effects are (1) the change in the adsorption characteristics of the ions present and (2) the shear plane position shifting away from the particle surface. In the situation of very low ion concentration, the first effect is negligible because the mobility is invariant with change of local ionic concentration.[27] It is the second effect that causes the ζ potential to change after copolymer adsorption. Thus, changes in the measured ζ potential are sensitive primarily to the adsorbed layer thickness and surface arrangement of the adsorbent. These in turn reflect the adsorbed chain density and chain conformation.

Data Interpretation. We infer from both time dependence of the adsorption process and the equilibrated states they produce (Figures 2–9) that there are at least two distinct adsorption states. The particles in one state, designated as state A, have a broad distribution of high mobilities. The particles in the other state, designated as state B, have a narrow distribution of low mobilities. All particles are initially in state A. They are partially or fully converted to state B during the kinetic process. The process for the initial adsorption must occur faster than our initial time scale of a few minutes. With the present setup and sample preparation procedure, we were not able to observe the initial encounter of copolymer micelles with the bare PSL particles. A stopped-flow device and a modification of the sample chamber may be needed in order to observe the initial adsorption process.

Thus, in our measurements, state A and state B are coexistent even at the earliest times we can observe after mixing. For the L69 particles, state A disappears after equilibrium, leaving the particles all in state B. For the L223 particles, the two states are always coexistent and there may or may not be a dynamic equilibration between the two states. From the present electrophoretograms, we are not able to distinguish the adsorbed particle size difference between the two states from the peak widths without independently knowing the mobility distributions. However, in an earlier dynamic light scattering study of another mixture,[10] we did find that the average particle diameter increased up to 10–20% over a period of 1 day. In Figure 4, the solid line, acquired 5 min after mixing, has two broad peaks originating from polydisperse mobility. The contribution of Brownian broadening to the linewidth for the L223 particles would be smaller (compare with the pure micelle peak, the thin line). After a few hours, both peaks become slimmer, indicating the mobility has become more homogeneous. However, the lower mobility peak (the right one) has a smaller linewidth than that of the higher one, indicating that in state A the adsorbed particles have either a smaller size or a higher polydispersity in mobility than that of the particles in state B. The size difference between the two states is too small to be seen in the size distribution resolved from the ill-conditioned Laplace inversion of the intensity–intensity autocorrelation function from dynamic light scattering. However, their mobility difference is much larger. Therefore, only after these electrophoretic light scattering experiments had been carried out, in which the peaks are separated by the ζ potential instead of by size, did we realize that the increase in average diameter observed previously actually originated from a competition between the two adsorption states. Such information could not be obtained from dynamic light scattering measurement results alone.

The ζ potentials of a particle before and after adsorption are related according to a simplified formulation:

$$\tanh\left(\frac{ze\zeta}{4k_BT}\right) \approx \tanh\left(\frac{ze\zeta_0}{4k_BT}\right)\exp(-\kappa\Delta) \tag{7}$$

where ζ and ζ_0 are the ζ potentials of adsorbed and unadsorbed particles, respectively, and Δ is the adsorbed layer thickness.[28] From eq 7 we learn that when particles are converted from state A to state B, they must have a thicker adsorption layer and, possibly, a denser structure.

Direct Micelle-Adsorption Model. In the direct micelle-adsorption model,[11] we predicted that when PSL particles are mixed with copolymers in a selective solvent, in which the A blocks have a weak affinity for the particle surface, direct micelle-adsorption will dominate the adsorption process, although there will also be unimer adsorption.

Let us consider the following three-step mechanism: (1) a reversible collisional process of adsorption–desorption of micelles onto the latex surface, (2) a surface rearrangement of the adsorbed micelles, and (3) formation of the final adsorbed layer by disruption of the micelle structure and contact of the PS core with the surface.

Step 1 would be controlled by diffusion of the two types of spheres and by the strength of the micelle-surface attachment. As predicted by a two-body collision theory, the adsorption process should be faster for particle pairs whose difference in size is large; i.e., this process should have a minimum rate for equal-size particles and a maximum rate for a small particle colliding with a flat surface. Although in our systems the sizes of micelles are much smaller than those of lattices, the differences in latex sizes are still expected to affect the adsorption process. On the other hand, desorption should be easier for the systems where the micelle-surface attachment is weaker, i.e., when micelles are attached to the surface by

(25) Xu, R.; Winnik, M. A.; Hallett, F. R.; Riess, G.; Croucher, M. D. *Macromolecules* **1991**, *24*, 87.
(26) Xu, R. *Langmuir* **1993**, *9*, 2955.
(27) Koopal, L. K.; Lyklema, J. *Discuss. Faraday Soc.* **1975**, *59*, 230.
(28) Fleer, G. J.; Koopal, L. K.; Lyklema, J. *Kolloid Z.-Z. Polym.* **1972**, *250*, 689.

fewer EO segments. Obviously, one can envisage that on small PSL particles micelles will have fewer attached segments since an increase of these types of interactions would imply a large increase in the elastic deformation energy of the micelles. This penalty would not be so significant for flat surfaces where micelles can contact more points on the surface without extensive deformation. Thus, micelles adsorbed on large particles will have a smaller desorption rate.

Once the micelles have attached onto the surface, their surface mobility can be due either to consecutive adsorption–desorption processes or to a surface migration process, or both. This migration process would be achieved by a "rolling over" of the adsorbed micelles promoted by "pushes" of other micelles in collision route toward the surface. With the same arguments as above, the desorption and the "rolling" processes would be easier for smaller PSL particles. Consequently, dense packing would be more quickly attained. On larger PSL particles, this process is more difficult and the micelle packing would be more randomlike.

These two steps are similar in nature and may be indistinguishable. The main conclusion to draw from these insights is that for small PSL particles the micelle-rearrangement process (not its disruption) is fast, leading to dense sphere packing on the latex surface, whereas for large PSL particles, this process is slower, leading to a random sphere packing with empty surface patches.

The adsorbed micelles to adsorbed chain transformation (AMACT) occurs in the third step. Since the relative affinity of PS is much stronger than that of PEO for the PS surface, to minimize the free energy, it will be favorable for the PS core of the adsorbed micelle to replace the PEO corona on the PS surface. For the PS core of a micelle to contact the surface, a considerable micelle deformation is required. On surfaces of small curvature, as the micelle suffers further deformation, the elastic penalty is more effectively compensated by the formation of more EO-surface attachments, whereas for small PSL particles the formation of new attachments, for the same deformation, is smaller. Therefore, the time scale for the AMACT process to occur could be several orders of magnitude faster when micelles on large PSL particles are compared to those on small PSL particles. It is even possible that the rate of this process might become comparable to the rates of the first two steps for micelles on larger PSL particles. In this case, dense packing would never be achieved.

Our study of electrophoretic mobilities of various mixtures supports the direct micelle-adsorption model and the three-step mechanism. Assuming that the hydrophobic PS core of micelle is solvent-free in aqueous solution, one can estimate from the aggregation number that the micelle core diameter is ca. 6 nm. As we have reported elsewhere, the ZGH3, ZGH4, and ZGH5 micelles have average hard-sphere-equivalent diameters ($2R_H$) of 40, 52, and 60 nm, respectively.[11] We present a pictorial view of this mechanism in Figure 10. On the left side we show the interaction of the micelles with a small PSL particle like L69. Here the first two steps are dominant over the last step; before those adsorbed micelles undergo AMACT, more micelles from solution come and push the adsorbed micelles away (rolling) in order for them to get in (route a'); in addition, that large curvature provides ample space for more micelles to approach the surface (route b'). Even for the PSL particles on which the micelles have gone through the AMACT there may still be bare patches with sufficient space for new comers (route c'). Through any one of the three routes, a dense packing is achievable. With more and more micelles (or unimers) squeezed onto a surface, the PEO chains of the adsorbed

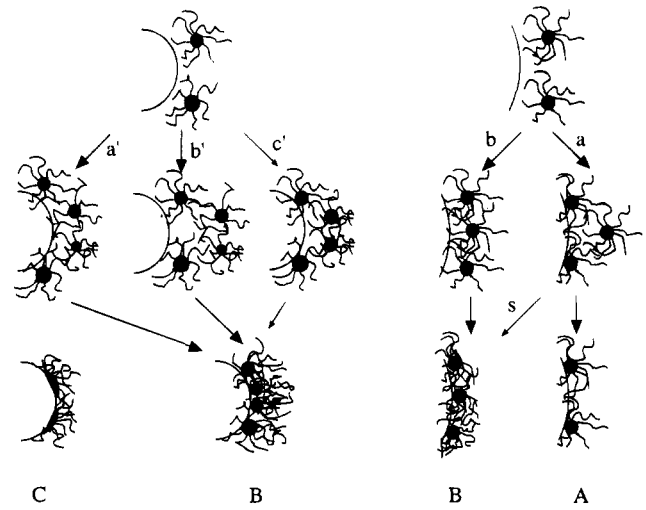

Figure 10. Cartoon depicting the processes for PEO-PS copolymer micelles adsorbing onto PSL particles. The left side is for adsorption onto small particles. After two micelles approach the surface, two subsequent micelles are able to adsorb regardless of the first two having adsorbed (a' and b') or not (c'). For larger particles (the right side), once the first two have adsorbed and their PEO chains have spread on the surface, there is no free surface available for the third one and it cannot adsorb (a), or adsorbs very slow (s), unless it comes before the first two have gone through the AMACT (b). Therefore, the two states (A and B) coexist. In the drawing, the adsorbed micelles in states A and B are still drawn as spheres for simplicity. In reality, we have observed that the micellar cores open up (melt down) on the surface so that PS blocks can have maximum contact with the surface as described in state C.[11]

Table 3. Mixing Ratio $W_c/(W_c + W_l)$ Needed To Reach Critical Coverage

sample	ZGH3	ZGH4	ZGH5
L69	0.33	0.33	0.38
L109C	0.18	0.18	0.21
L223	0.07	0.07	0.08

micelles become stretched out and brushlike, and the adsorption layer becomes thicker and more dense. Consequently, the measured electrophoretic mobility starts with a broad distribution. As the adsorption process proceeds along the three routes, the electrophoretic mobilities become smaller and more monodisperse as the system approaches equilibrium.

According to our model, the number of block copolymer chains adsorbed per unit area (σ) is related to the latex diameter d_L, the micelle aggregation number f, and an angle α that is related to the ratio of the micelle diameter to d_L:[11]

$$\sigma(\text{chain/nm}^2) = \frac{2f}{(3\alpha - \pi)d_L^2} \qquad (8)$$

Although this number is not the maximum value for single-layer adsorption, it gives an estimate based on steric consideration related to packing micelle spheres on hard-sphere surfaces. However, in Figures 7–9, even for mixing ratios much higher than the values listed, there are still changes in mobility peak position as the mixing ratio increases. This is an indirect indication that there does exist a dynamic equilibrium between the adsorbed micelles and free micelles. σ can also be considered as a critical coverage value, which can be identified with the crossover from the region where individual adsorbed micelles do not interact with each other to the region where this interaction is significant. Table 3 lists the mixing ratio needed to satisfy this equation if all micelles in solution

are adsorbed. For surface coverage values below the critical point the AMACT process would be achieved exclusively by independent disruption of individual micelles, and the final packing of the chain in the adsorbed layer should be train-loop-tail-like, leading always to a single population. This is the case for the systems ZGH3+L69 (Figures 2 and 5) and ZGH4+L69 (Figure 3). The disappearance of the high-mobility shoulder in Figures 2 and 3 would then be due to the progressive and slow disappearing of the micelle-surface structure and the rise of the mushroomlike chain-surface structure accompanying further adsorption. The shift in the peak observed in Figure 5 is due to a less patchy surface as the coverage increases and a more efficient screening by PS blocks as opposed to a slight screening by the PEO blocks. Beyond the critical coverage value, one can envisage an AMACT involving a cooperative process propagating to the whole latex surface. According to our model for small particles, the surface will be densely packed and homogeneously covered. The AMACT process would be the only one observed, leading once again to a single mobility population.

For large particles, the adsorbed micelles have less surface mobility. After the initial adsorption, in which the adsorbed micelle number is related to the mixing ratio, there would not be enough space outside of the adsorbed layer for micelles in solutions to approach the surface. In our view, they are blocked by the steric barrier of the previously adsorbed block copolymers. Furthermore, on a flat surface, the AMACT may occur on the same time scale as the first two steps. Then route a would dominate over route b in Figure 10, leading to a patchy surface. Once the first "tide" of micelles has occupied the surface, subsequently micelles have to either adsorb onto whatever free surface is left (route a) or replaced the adsorbed chains. The replacement may be slow and inefficient. It has been reported that, even for a single stronger adsorbing polymer to replace an adsorbed polymer, the process may have a time scale on the order of weeks. In addition, polymer desorption by such replacement occurs segment by segment.[29] For larger PSL particles, although the process labeled s in Figure 10 is possible, it is inevitably very slow. Therefore, some particles, beyond the critical coverage, will undergo a cooperative process, giving rise to one type of population with low electrophoretic mobility, whereas the other particles, behind the critical point, will suffer a noncooperative AMACT process, giving rise to a different type of surface population with latexlike mobility. Only in this way can we explain why there are always two mobility populations for the L223 particles. Our model also suggests that the larger the particle size, the faster the AMACT process, producing a looser and patchier layer. This explains why, when there are two peaks, the mobility of the higher mobility peak for the L223 particles is higher than that of the L109C particles.

For the purpose of discussion, let us define t' as the AMACT relaxation time. We anticipate that t' would be larger for large micelles when compared with small ones adsorbing onto the same PSL particles, i.e., $t'_{ZGH5} > t'_{ZGH4} > t'_{ZGH3}$. A larger t' means that more adsorption would go to route b, resulting in less or minimum adsorption in state A. Consequently, the transition observed for the system L109+ZGH3 going from two peaks to one peak reflects a transition between a situation where both types of AMACT are possible to the situation where the cooperative process dominates. For larger micelles (ZGH4 and ZGH5) t' is so big that route b dominates over route a. The micelles are more loose on the surface, and the dense packing situation is more favored; the superposition of the two regions might never be observed.

There is a common feature in Figures 7–9: at high micelle mixing ratios the mobility of the lower mobility peak for adsorbed L223 particles is lower than that of adsorbed L69 particles and very close to zero mobility. We propose a possible explanation as follows. The particle size of L223 particles in the presence of block copolymer calculated from the translational diffusion coefficient by dynamic light scattering measurements is indistinguishable from, sometimes even smaller than, that a bare L223 particles.[30] A similar phenomenon was reported recently on PSL particles in dilute aqueous solution.[31] Johnson found that PSL particles in water have an average 6% expansion in diameter containing ~15 wt % of water due to hydration. The adsorption of neutral polymer such as Triton-100 should increase the PSL diameter. However, in the presence of 0.01 M NaCl, the diameter increase disappeared, although sedimentation experiments indicated that adsorption did take place. Johnson attributed this observation to strengthening of hydrophobic bonding tendencies and packing down of the hydrophobic portion of the molecules on the PS surface.

In our systems, although there is no added electrolyte, the adsorbed PS portion as well as the PEO portion in state B are likely densely packed down on the surface and the particles are partially dehydrated. This process effectively "buries" or "shields" most of the surface charges. The particles with adsorbed copolymer then behave like more neutral ones. The same behavior would be expected for the L69 and L109C systems as well, but this process may be less effective because of the stretched brushlike PEO chains. To further verify the adsorption kinetics, it would be necessary to use sedimentation or classical light scattering techniques to measure the particle weight change during adsorption.

Acknowledgment. The authors wish to thank Ms. Tetje Jensma for preparing the micelle solution. R.X. thanks Coulter Corp. for its support. M.A.W. thanks the NSERC of Canada for financial support. J.M.G.M. thanks the JNICT for financial support.

(29) van der Beek, G. P.; Cohen Stuart, M. A.; Fleer, G. J. *Macromolecules* **1991**, *24*, 3553.

(30) d'Oliveira, J. M. R. Ph.D. Dissertation, Technical University of Lisbon, Portugal, 1993.

(31) Johnson, P. *Langmuir* **1993**, *9*, 2318.